Available online at www.sciencedirect.com
ScienceDirect
Free Radical Biology & Medicine 41 (2006) 1338–1350
www.elsevier.com/locate/freeradbiomed

Original Contribution

A New Paradigm: Manganese Superoxide Dismutase Influences the Production of H_2O_2 in Cells and Thereby Their Biological State

Garry R. Buettner [a,*], Chin F. Ng [b], Min Wang [a], V.G.J. Rodgers [b], Freya Q. Schafer [a]

[a] *Free Radical and Radiation Biology Program, EMRB 68, The University of Iowa, Iowa City, IA 52242-1101, USA*
[b] *Chemical and Biochemical Engineering, The University of Iowa, Iowa City, IA 52242, USA*

Received 8 March 2006; revised 9 June 2006; accepted 14 July 2006
Available online 21 July 2006

Abstract

The principal source of hydrogen peroxide in mitochondria is thought to be from the dismutation of superoxide *via* the enzyme manganese superoxide dismutase (MnSOD). However, the nature of the effect of SOD on the cellular production of H_2O_2 is not widely appreciated. The current paradigm is that the presence of SOD results in a lower level of H_2O_2 because it would prevent the non-enzymatic reactions of superoxide that form H_2O_2. The goal of this work was to: a) demonstrate that SOD can increase the flux of H_2O_2, and b) use kinetic modelling to determine what kinetic and thermodynamic conditions result in SOD increasing the flux of H_2O_2. We examined two biological sources of superoxide production (xanthine oxidase and coenzyme Q semiquinone, $CoQ^{\bullet-}$) that have different thermodynamic and kinetic properties. We found that SOD could change the rate of formation of H_2O_2 in cases where equilibrium-specific reactions form superoxide with an equilibrium constant (K) less than 1. An example is the formation of superoxide in the electron transport chain (ETC) of the mitochondria by the reaction of ubisemiquinone radical with dioxygen. We measured the rate of release of H_2O_2 into culture medium from cells with differing levels of MnSOD. We found that the higher the level of SOD, the greater the rate of accumulation of H_2O_2. Results with kinetic modelling were consistent with this observation; the steady-state level of H_2O_2 increases if $K<1$, for example $CoQ^{\bullet-}+O_2 \rightarrow CoQ+O_2^{\bullet-}$. However, when $K>1$, *e.g.* xanthine oxidase forming $O_2^{\bullet-}$, SOD does not affect the steady state-level of H_2O_2. Thus, the current paradigm that SOD will lower the flux of H_2O_2 does not hold for the ETC. These observations indicate that MnSOD contributes to the flux of H_2O_2 in cells and thereby is involved in establishing the cellular redox environment and thus the biological state of the cell.

Keywords: Superoxide dismutase; Mitochondria; Coenzyme Q; Hydrogen peroxide; Superoxide; Redox environment; Free radical

Introduction

Superoxide dismutase is an important antioxidant enzyme as it is found in nearly all organisms. In mammals there are at least three forms of SOD: a cytosolic (CuZnSOD), an extracellular (ECSOD), and a mitochondrial form (MnSOD). All SOD enzymes catalyze the dismutation of superoxide, Reactions (2)–(5) Table 1 [1,2]:

$$O_2^{\bullet-} + O_2^{\bullet-} + 2H^+ \xrightarrow{\text{SOD } k \approx 2\times10^9 M^{-1}s^{-1}} H_2O_2 + O_2$$

[3–5]

It has been shown that MnSOD-knockout mice die within 1–18 days after birth, depending on their genetic background [6,7]; thus, MnSOD is an essential enzyme. Changes in SOD levels inside cells can have opposing effects. High over-expression of SOD in *E. coli* has been found to increase sensitivity to paraquat and to hyperoxia [8], as well as ionizing radiation due to apparent increased production of H_2O_2 [9]. Human and mouse cell clones that overexpress human CuZnSOD appear to have higher levels of hydrogen peroxide [10,11]. However, transfection of V79 Chinese hamster cells to overexpress CuZnSOD resulted in a decrease in H_2O_2 in cells [12]. Overexpression of MnSOD in several human cell lines has provided indirect evidence that this increased expression leads to increases in the production of H_2O_2 [13–16]. However, the current paradigm in the research community is that SOD decreases the production of H_2O_2

* Corresponding author. Fax: +1 319 335 9112.
E-mail address: garry-buettner@uiowa.edu (G.R. Buettner).

0891-5849/$ - see front matter © 2006 Elsevier Inc. All rights reserved.
doi:10.1016/j.freeradbiomed.2006.07.015

Table 1
The reactions in the kinetic model

Reaction number	Reaction	Rate constant $M^{-1}\cdot s^{-1}$ or s^{-1}	Reference/comment
1a	$XO\text{-}FADH^{\bullet}+O_2 \rightarrow XO\text{-}FAD+O_2^{\bullet-}+H^+$	$k_{1a}=7\times10^4$	[30]
−1a	$XO\text{-}FAD+O_2^{\bullet-}+H^+ \rightarrow XO\text{-}FADH^{\bullet}+O_2$	$k_{-1a}=7$	Estimated here using $K_{1a}=10^4$
1b	$CoQ_{10}^{\bullet-}+O_2 \rightarrow CoQ_{10}+O_2^{\bullet-}$	$k_{1b}=8\times10^3$	[74,92–94] The actual value is uncertain, but an equilibrium constant appears to be ≈0.01–0.1.
−1b	$CoQ_{10}+O_2^{\bullet-} \rightarrow CoQ_{10}^{\bullet-}+O_2$	$k_{-1b}=8\times10^5$	[74,92,93]
2	$Mn^{III}SOD+O_2^{\bullet-} \rightarrow Mn^{III}SOD{:}O_2^{\bullet-}$ [a]	$k_2=1.5\times10^9$	[96,97]
−2	$Mn^{III}SOD{:}O_2^{\bullet-} \rightarrow Mn^{III}SOD+O_2^{\bullet-}$	$k_{-2}=3.5\times10^4$	[96]
3	$Mn^{III}SOD{:}O_2^{\bullet-} \rightarrow Mn^{II}SOD+O_2$	$k_3=2.5\times10^4$	[96]
−3	$Mn^{II}SOD+O_2 \rightarrow Mn^{III}SOD{:}O_2^{\bullet-}$ [a]	$k_{-3}=0$	[96]
4	$Mn^{II}SOD+O_2^{\bullet-} \rightarrow Mn^{II}SOD{:}O_2^{\bullet-}$ [b]	$k_4=1.5\times10^9$	[95,96]
−4	$Mn^{II}SOD{:}O_2^{\bullet-} \rightarrow Mn^{II}SOD+O_2^{\bullet-}$	$k_{-4}=3.5\times10^4$	[96]
5	$Mn^{II}SOD{:}O_2^{\bullet-}+2H^+ \rightarrow Mn^{III}SOD+H_2O_2$	$k_5=2.5\times10^4$	[96]
−5	$Mn^{III}SOD+H_2O_2 \rightarrow Mn^{II}SOD{:}O_2^{\bullet-}+2H^+$	$k_{-5}=300$	[96]
6	$Mn^{II}SOD{:}O_2^{\bullet-} \rightarrow DEP$ [c]	$k_6=650$	[96]
−6	$DEP \rightarrow Mn^{II}SOD{:}O_2^{\bullet-}$	$k_{-6}=10$	[96]
7	$2H^++2O_2^{\bullet-} \rightarrow O_2+H_2O_2$	$k_7=2.4\times10^5$	[5]
−7	$O_2+H_2O_2 \rightarrow 2H^++2O_2^{\bullet-}$	$k_{-7}=0$	[5]
8	$GPx_r+H_2O_2+H^+ \rightarrow GPx_0+H_2O$ [d]	$k_8=2.1\times10^7$	[97–99]
−8	$GPx_0+H_2O \rightarrow GPx_r+H_2O_2$	$k_{-8}=0$	[97,98]
9	$GPx_0+GSH \rightarrow GSGPx+H_2O$	$k_9=4\times10^4$	[97,98]
−9	$GSGPx+H_2O \rightarrow GPx_0+GSH$	$k_{-9}=0$	[97,98]
10	$GSGPx+GSH \rightarrow GPx_r+GSSG+H^+$	$k_{10}=1\times10^7$	[97,98]
−10	$GPx_r+GSSG+H^+ \rightarrow GSGPx+GSH$	$k_{-10}=0$	[97,98]
11	$GSSG \rightarrow 2GSH$		
−11	$2GSH \rightarrow GSSG$		
12	$CoQ^{\bullet-}+O_2^{\bullet-}+2H^+ \rightarrow CoQ+H_2O_2$	$k_{12(obs)}=3\times10^6$ [e]	Estimated

[a] $Mn^{III}SOD{:}O_2^{\bullet-}$ is a complex of $Mn^{III}SOD$ and $O_2^{\bullet-}$.
[b] $Mn^{II}SOD{:}O_2^{\bullet-}$ is a complex of $Mn^{II}SOD$ and $O_2^{\bullet-}$.
[c] DEP is dead end product.
[d] Catalase was not included in the kinetic model because it is primarily a peroxisomal enzyme. We included only GPx1 as a sink for H_2O_2. Because we kept the capacity of the system for removing H_2O_2 constant, the inclusion of catalase or peroxiredoxin-III as additional components of the H_2O_2-removing system would make no difference in the final results of the model.
[e] This is an estimate based on the non-enzymatic dismutation of superoxide. The rate constant will rely on the pH and pK_a of these two species. If we assume the maximum rate constant is parallel to that of superoxide, *i.e.* the reaction of protonated and unprotonated species, then we can assume that the fastest reaction will have either $O_2^{\bullet-}$ protonated or $CoQ^{\bullet-}$ protonated. If the effective pK_a of $CoQH^{\bullet}$ is 5.9 [100] then at pH 7.4 about 3% of $CoQ^{\bullet-}$ and 0.2% of $O_2^{\bullet-}$ will be protonated. With this, an estimate of an observed rate constant would be $k_{obs}\approx3\times10^6\ M^{-1}\ s^{-1}$. Once superoxide is formed, possible routes to formation of H_2O_2, as a rate equation, are: $+d[H_2O_2]/dt=\{k_{SOD}\ [SOD]+k_{CoQ^{\bullet-}}\ [CoQ^{\bullet-}]+k_{dismut}[O_2^{\bullet-}]+k_{other}[other]\}\ [O_2^{\bullet-}]$. Estimating the contributions of each term $+d[H_2O_2]/dt=\{2\times10^4\ s^{-1}+3\times10^{-1}\ s^{-1}+2.4\times10^{-4}\ s^{-1}\times+k_{other}[other]\}\times[O_2^{\bullet-}]$, and assuming that $[O_2^{\bullet-}]$ is at most on the order of 1 nM, we see that the termination reaction in question is negligible, as well as the chemical dismutation of superoxide. Thus this reaction was not included in the kinetic model. Here, "other" refers to reactions of superoxide with substances such as aconitase, Fe^{3+}cytochrome *c*, nitric oxide. These represent a small fraction of the reactions of superoxide [101,102].

[17–19]: "the proposal that SOD enhances H_2O_2 by catalyzing the dismutation reaction can be discounted" [17].

The current paradigm

The concentrations of $O_2^{\bullet-}$ and H_2O_2 in a cell are assumed to be in a quasi steady-state. These steady-state concentrations, $[O_2^{\bullet-}]_{ss}$ and $[H_2O_2]_{ss}$, reflect a balance between the rate of formation and the rate of removal. Thus, the steady-state level can change by either changing the rate of formation and/or the rate of removal. It is widely accepted that changes in levels of cellular SOD will result in:

a. a change in $[O_2^{\bullet-}]_{ss}$, *e.g.* an increase in SOD would increase the rate of removal of $O_2^{\bullet-}$ and thereby lower $[O_2^{\bullet-}]_{ss}$;
b. no change in the rate of production of $O_2^{\bullet-}$;
c. a minor change in the rate of production of H_2O_2, no more than a factor of two (This assumes that *Case 3* described below is not applicable.); this change in the rate of production of H_2O_2 could result in
d. a minor change in $[H_2O_2]_{ss}$ [17].

This paradigm is based on the observation that the rate of production of H_2O_2 by the enzyme xanthine oxidase (XO) is not affected by SOD. XO is a well-studied enzyme that is widely used as a tool to generate superoxide and hydrogen peroxide in experimental systems [20].

A new paradigm

However, we propose that there are other superoxide-generating systems (*e.g.* the mitochondrial electron transport

chain) that do not behave like the xanthine/xanthine oxidase (X/XO) system. In these systems, changes in levels of cellular SOD can result in:

a. a change in $[O_2^{\bullet -}]_{ss}$;
b. a change in the rate of production of $O_2^{\bullet -}$;
c. a major change in the rate of production of H_2O_2, more than a factor of two; this could result in
d. a major change in $[H_2O_2]_{ss}$.

How could SOD change the level of H_2O_2 in cells?

There are various ways that superoxide can be converted to H_2O_2.

Case 1: Dismutation reaction

Independent of how $O_2^{\bullet -}$ dismutes, *i.e.* with or without SOD, two $O_2^{\bullet -}$ will yield one H_2O_2, net of Reactions (2)–(5) of Table 1.

Case 2: Reactions with electron donors

If $O_2^{\bullet -}$ reacts with an electron-proton/hydrogen-atom donor, then one $O_2^{\bullet -}$ will yield one H_2O_2.

$$O_2^{\bullet -} + \text{donor-H} + H^+ \rightarrow H_2O_2 + \text{donor}^{\bullet}$$

In addition to cellular reducing agents, the donor could be a transition metal such as Fe^{2+} yielding Fe^{3+}, for example with the 4Fe–4S cluster of aconitase.

Case 3: Chain reactions that produce superoxide

There are cases where one superoxide can result in the formation of considerably more of both superoxide and hydrogen peroxide, *i.e.,* one $O_2^{\bullet -}$ will yield n H_2O_2, where n can be much greater than one. This scenario can occur in a chain reaction where $O_2^{\bullet -}$ is a product of the reaction and is also a chain-carrying radical, initiating a new chain [21–24].

An example is the oxidation of 6-hydroxydopamine (6-OHDA) to its semiquinone ($SQ^{\bullet -}$) and quinone (Q):

$$\text{6-OHDA} + Fe^{3+} \rightarrow SQ^{\bullet -} + Fe^{2+} \text{(Initiation)}$$

$$SQ^{\bullet -} + O_2 \rightarrow Q + O_2^{\bullet -} \text{(Superoxide formation)}$$

$$\text{6-OHDA} + O_2^{\bullet -} \rightarrow SQ^{\bullet -} + H_2O_2 \text{(Chain propagation)}$$

$$SQ^{\bullet -} + O_2^{\bullet -} + 2H^+ \rightarrow Q + H_2O_2 \text{(Chain termination)}$$

$$2SQ^{\bullet -} + 2H^+ \rightarrow \text{6-OHDA} + Q \text{(Chain termination)}$$

$$O_2^{\bullet -} + O_2^{\bullet -} + 2H^+ \rightarrow O_2 + H_2O_2 \text{(Termination)}$$

Here, after initiation, $O_2^{\bullet -}$ is formed by electron transfer from the semiquinone radical of 6-OHDA ($SQ^{\bullet -}$) to O_2. Superoxide then serves as a chain-carrying radical to initiate additional oxidation cycles, each forming another $O_2^{\bullet -}$ and H_2O_2. Thus, the formation of one $O_2^{\bullet -}$ will lead to n H_2O_2, where n is essentially the chain-length of this set of reactions. The chain termination reaction of $SQ^{\bullet -} + O_2^{\bullet -}$ is probably not of consequence. See Table 1. Iron(III) is shown as the initiating species above, but in higher pH environments metals may not be needed as true autoxidation can occur [25].

Case 4: Reactions with non-hydrogen atom electron acceptors/donors

If superoxide reacts with an electron-acceptor, such as Fe^{3+}cytochrome *c*, or covalently with an electron-donor, such as nitric oxide, then there will be no H_2O_2 produced. In this case, SOD would increase the rate of production of H_2O_2. Although these reactions of superoxide are biologically important, they were not included in this study as they are typically minor sinks for superoxide. In addition, the reactions are not considered reversible, and the focus of this study is on the *reversible formation* of superoxide and subsequent formation of hydrogen peroxide.

The current paradigm is that if SOD is present in *Cases* 2 and 3 above, its reaction with $O_2^{\bullet -}$ would dominate reactions of $O_2^{\bullet -}$ with donor-H or the chain-initiation by $O_2^{\bullet -}$, thereby converting these processes into *Case* 1, resulting in less H_2O_2. In *Case* 2 the amount of H_2O_2 would decrease by no more than a factor of two; in *Case* 3 the decrease would be by a factor of approximately n. In these cases, SOD lowers the level of H_2O_2. Translating this into a cellular setting would mean that overexpression of SOD in cells would result in lower levels of H_2O_2. However, experimental data have provided indirect evidence that cells with increased levels of SOD can have increased levels of H_2O_2 [13–16]. This apparent contradiction can be rationalized if increasing SOD increases the rate of formation of $O_2^{\bullet -}$ and consequently H_2O_2. The paradigm summarized above does not consider the possibility that SOD could change the rate of production of $O_2^{\bullet -}$ by reversible reactions.

How could SOD change the rate of formation of $O_2^{\bullet -}$ and H_2O_2?

If the rate of production of $O_2^{\bullet -}$ in a system is constant and the amount of SOD varies, then as indicated above the rate of production of H_2O_2 will either remain the same, Case 1, or decrease, Cases 2 and 3. However, if Le Chatelier's principle[1] applies to the reaction forming $O_2^{\bullet -}$, then the rate of production of $O_2^{\bullet -}$ could change with changing levels of SOD, resulting in an increase in the rate of production of H_2O_2.

For example, in the reaction below, if SOD is present it will compete with the reverse reaction and remove some of the $O_2^{\bullet -}$ and thereby "pull" the reaction to the right. SOD will have the

[1] Le Chatelier's Principle states that if the conditions of a system, initially at equilibrium, are changed, the equilibrium will shift in such a direction as to tend to restore the original conditions.

most influence when the rate constant of the reverse reaction is greater than the rate constant of the forward reaction ($k_r > k_f$; $K = k_f/k_r < 1$).

$$Y^{\bullet -} + O_2 \underset{k_r}{\overset{k_f}{\rightleftharpoons}} Y + O_2^{\bullet -} \qquad K < 1$$

Increased levels of SOD will pull the equilibrium of this reversible reaction to the right, and the rate of production of $O_2^{\bullet -}$ and subsequently H_2O_2 will increase. If the reverse reaction is slow ($k_r < k_f$; $K > 1$),

$$Y^{\bullet -} + O_2 \underset{k_r}{\overset{k_f}{\rightleftharpoons}} Y + O_2^{\bullet -} \qquad K > 1$$

then only a very small fraction of the $O_2^{\bullet -}$ molecules will enter the reverse reaction and dismutation will occur with or without SOD. Changes in the amount of SOD would have little impact. In a cellular setting both scenarios can be found. In the case of XO ($K > 1$) we propose that the current paradigm applies, *i.e.* increasing SOD will either have no effect, *Case 1*, or decrease levels of H_2O_2, because the rate of the reverse reaction is slow compared to the forward reaction that produces $O_2^{\bullet -}$, *i.e. Case 2*. However, there are reactions in the cell that have $K < 1$, for example $CoQ^{\bullet -}$ forming $O_2^{\bullet -}$. We propose that when the reverse reaction is comparable to or faster than the forward reaction ($K < 1$), then Le Chatelier's principle may apply and the current paradigm no longer holds. Or stated another way, when the equilibrium constant (K) for the reaction forming $O_2^{\bullet -}$ is $\gg 1$, then SOD will have little effect on the rate of production of H_2O_2; but, when K is ≈ 1 or < 1, then SOD can affect the rate of production of H_2O_2. We propose that the latter is the case in the $CoQ^{\bullet -}$ reaction, but not in the reaction of XO to form $O_2^{\bullet -}$.

The xanthine oxidoreductase system, thermodynamics

The metalloenzyme xanthine oxidoreductase (XOR) is a dimer that contains two molybdenum (Mo) atoms and eight irons as four (2Fe–2S) moieties. In addition there are two FAD groups in the enzyme. Thus, each subunit contains, 1 Mo, 2 (2Fe–2S), and 1 FAD [26]. The oxidase form of XOR is a widely used tool to produce superoxide in the laboratory, but it can also be a major source of unchecked superoxide production *in vivo* [27,28]. The oxidase form (XO) oxidizes xanthine, hypoxanthine or other substrates using oxygen as the preferred electron-acceptor, producing $O_2^{\bullet -}$ and H_2O_2, Fig. 1 [29–31].

$$\text{Xanthine} + O_2 \overset{\text{XO}}{\rightleftharpoons} \text{uric acid} + O_2^{\bullet -} + H_2O_2.$$

It is the radical of the flavin moiety (XO-FADH$^{\bullet}$) that interacts with O_2 forming $O_2^{\bullet -}$ and subsequently H_2O_2 [32].

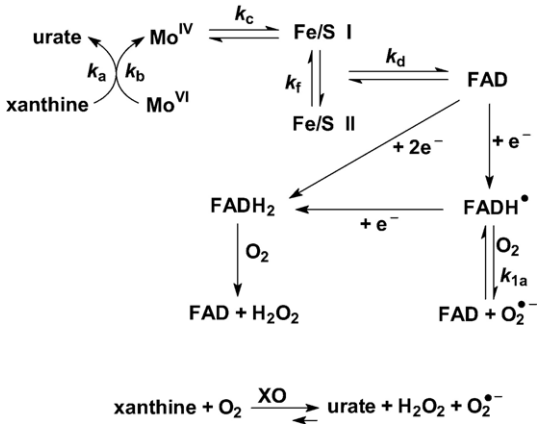

Fig. 1. The flow of electrons through xanthine oxidase. Xanthine makes a complex with XO at the molybdenum site ($k_a = 6 \times 10^6$ M^{-1} s^{-1}, 37 °C); then xanthine is oxidized to urate with reduction of the molybdenum ($k_b = 15$ s^{-1}). This is followed by transfer of electrons to the Fe/S centers ($k_c = 8.5 \times 10^3$ s^{-1}); then to FAD ($k_d = 2 \times 10^2$ s^{-1}), and finally production of $O_2^{\bullet -}$ from FADH$^{\bullet}$ ($k_{1a} = 7 \times 10^4$ M^{-1} s^{-1}). The thermodynamics for the formation of $O_2^{\bullet -}$ from the FADH$^{\bullet}$ indicate an equilibrium constant of $\approx 10^4$. Thus the back reaction would have a rate constant of ≈ 7 M^{-1} s^{-1} [30].

(The direct two-electron reduction of oxygen to form H_2O_2 in general occurs through a fully reduced flavin, $FADH_2$).

$$\text{XO-FADH}^{\bullet} + O_2 \overset{K_{1a}}{\rightleftharpoons} \text{XO-FAD} + O_2^{\bullet -} + H^+$$

Reaction (1a)

The equilibrium constant for this reaction can be estimated from the reduction potentials of the two redox couples:

$$E^{\circ\prime}(\text{XO-FAD/XO-FADH}^{\bullet}; \text{pH } 7.4) = -400 \text{ mV}$$

[33,34]

$$E^{\circ\prime}(O_2/O_2^{\bullet -} \text{pH } 7.4) = -160 \text{ mV}$$

[35]

Using the fundamental relationship connecting the Gibbs free energy of a reaction to its equilibrium constant, *i.e.* $\Delta G^{\circ\prime} = -nF\Delta E^{\circ\prime} = -RT \ln K$, the equilibrium constant for the formation of $O_2^{\bullet -}$ by the flavin radical in XO is $\gg 1$ ($K_{1a} = 10^4$). With this equilibrium constant, very little of the $O_2^{\bullet -}$ produced will enter into the reverse reaction; in the absence of SOD the $O_2^{\bullet -}$ formed will chemically dismute. The addition of SOD would have little effect on the rate of production of H_2O_2. SOD would convert the chemical dismutation into a faster enzyme-catalyzed dismutation and thereby lower the steady-state level of $O_2^{\bullet -}$. However, it will not have a detectable effect on the production of H_2O_2 because there is not much superoxide entering into the reverse reaction to draw from.

The CoQ system, thermodynamics

The CoQ-system of the mitochondrial electron transport chain has a different equilibrium constant than the X/XO system for forming $O_2^{\bullet -}$. Superoxide is formed by

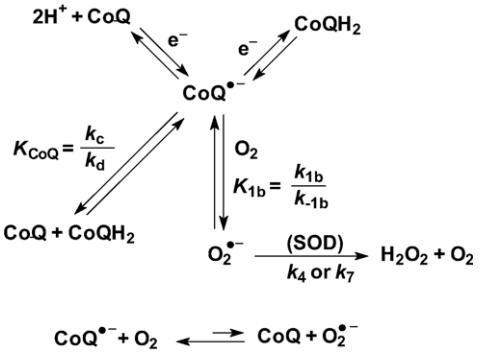

Fig. 2. $CoQ^{\bullet -}$ of the ETC can make $O_2^{\bullet -}$, a source of H_2O_2. $CoQ^{\bullet -}$ can be formed during electron/proton transfer during the protonmotive Q-cycle, from comproportionation of CoQ and $CoQH_2$, and also by other one-electron oxidation-reduction processes. K_{1b} is the equilibrium constant highlighted in the model. (k_c and k_d are the rate constants for comproportionation and disproportionation, respectively).

mitochondria [36–38]; a major source is thought to be $CoQ^{\bullet -}$, Reaction (1) (Table 1, Fig. 2) [39,40]:

$$CoQ^{\bullet -} + O_2 \overset{K_{1b}}{\rightleftharpoons} CoQ + O_2^{\bullet -} \qquad \text{Reaction (1b)}$$

Literature values for this one-electron reduction potential vary considerably due to the difficulty of determining a true reduction potential while in the membrane. Values range from −40 mV to −230 mV [35,41–43], depending on solvent, environment [44], and whether CoQ is bound. Thus, the one-electron reduction potential for CoQ is estimated as:

$$E^{\circ\prime}(CoQ/CoQ^{\bullet -}; \text{pH } 7.0) = -40 \text{ to } -230 \text{ mV}$$

[41,42,44]

Using this range of one-electron reduction potentials, the estimated equilibrium constant for Reaction (1b) is $K_{1b} \approx 10^{-2}$–10^{+1}, which is much smaller than $K_{1a} \approx 10^{+4}$ for the production of superoxide by the flavin radical in XO. Because of the relatively rapid reverse reaction for Reaction (1b), we propose that the current paradigm, that SOD has no influence on the rate of production, will not apply for the CoQ system. Modulating the level of SOD in the CoQ-system would result in a change in the net rate for the reaction forming $O_2^{\bullet -}$; following Le Chatelier's principle, an increase in MnSOD would change the rate of production of $O_2^{\bullet -}$ and H_2O_2.

To examine how the value of the equilibrium constant, K_1, alters the rate of formation of $O_2^{\bullet -}$ and subsequent production of H_2O_2 and how SOD influences the system, we developed a kinetic model to simulate the production of superoxide and hydrogen peroxide by the mitochondrial CoQ system and the X/XO-system.

Materials and methods

Kinetic model of the superoxide-peroxide system

Antioxidant enzymes are involved in a series of reactions, converting superoxide radical to hydrogen peroxide, and finally to water. Superoxide dismutases convert superoxide radical to hydrogen peroxide. Catalase and glutathione peroxidase on the other hand convert hydrogen peroxide to water. The reactions involved can be separated into three phases:

I. Superoxide generation

$$XO\text{-}FADH^{\bullet} + O_2 \rightleftharpoons XO\text{-}FAD + O_2^{\bullet -} + H^+ \qquad \text{Reaction (1a)}$$

$$CoQ^{\bullet -} + O_2 \rightleftharpoons CoQ + O_2^{\bullet -}. \qquad \text{Reaction (1b)}$$

II. Superoxide dismutation

$$O_2^{\bullet -} + O_2^{\bullet -} + 2H^+ \xrightarrow{(SOD)} H_2O_2 + O_2.$$

net Reactions (2)–(5) and Reaction (7)

III. Peroxide removal

$$2H_2O_2 \xrightarrow{\text{Catalase}} 2H_2O + O_2$$

$$H_2O_2 + 2GSH \xrightarrow{GPx} 2H_2O + GSSG.$$

When considering the complete process, from the generation of superoxide radicals to the final conversion of hydrogen peroxide to water inside mitochondria, a detailed version can be written as in Table 1. From these reactions a rate expression can be written for time-dependent concentration changes for each species, Table 2. The subsequent sixteen non-linear ordinary differential equations (ODE) are shown in Equations (15)–(30). Evaluating the reaction rate constants, these equations represent a stiff system. Therefore, the modified Rosenbrock numerical method was selected to solve the transient expressions [45].

H_2O_2 measurement from cells

To determine if cells with varying levels of MnSOD produce H_2O_2 at different rates, we measured the accumulation of H_2O_2 in their growth medium. The steady-state level of H_2O_2 in cells has been estimated to be in the range of 10^{-10}–10^{-7} M [46–49]; the levels are normally on the order of 10^{-9}–10^{-8} M (1–10 nM), with higher levels associated with pathology [48]. However, intracellular determination of levels of H_2O_2 is problematic. We relied on the diffusion of H_2O_2 from cells into culture medium. The diffusion coefficient of H_2O_2 is nearly the same as H_2O, but more importantly, their permeability coefficients to cellular membranes are also nearly the same [46,50]. The time constant for the exchange of intracellular water for glioma cells in culture is on the order of 50 ms [51]. While the equivalent time constant in the fully functioning brain *in vivo* is an order of magnitude larger [52], this time constant is still <1 s. Thus, intracellular H_2O_2 will rapidly appear in the extra-cellular medium. The rate of appearance is proportional to the concentration gradient between the inside and outside of the cell. The levels of H_2O_2 were measured by the change in fluorescence of Amplex Red,

Table 2
The differential equations of the model

$$\frac{d[CoQ_{10}^{\bullet-}]}{dt} = k_{-1}[CoQ_{10}][O_2^{\bullet-}] - k_1[CoQ_{10}^{\bullet-}][O_2] \quad (15)$$

$$\frac{d[CoQ_{10}]}{dt} = k_1[CoQ_{10}^{\bullet-}][O_2] - k_{-1}[CoQ_{10}][O_2^{\bullet-}] \quad (16)$$

$$\frac{d[O_2]}{dt} = k_{-1}[CoQ_{10}][O_2^{\bullet-}] + k_3[Mn^{III}SOD : O_2^{\bullet-}] + 2k_7[O_2^{\bullet-}]^2 - k_1[CoQ_{10}^{\bullet-}][O_2] \quad (17)$$

$$\frac{d[O_2^{\bullet-}]}{dt} = k_1[CoQ_{10}^{\bullet-}][O_2] + k_{-2}[Mn^{III}SOD : O_2^{\bullet-}] + k_{-4}[Mn^{II}SOD : O_2^{\bullet-}] - k_{-1}[CoQ_{10}][O_2^{\bullet-}] - k_2[Mn^{III}SOD][O_2^{\bullet-}] - k_4[Mn^{II}SOD][O_2^{\bullet-}] - 2k_7[O_2^{\bullet-}]^2 \quad (18)$$

$$\frac{d[Mn^{III}SOD]}{dt} = k_{-2}[Mn^{III}SOD : O_2^{\bullet-}] + k_5[Mn^{II}SOD : O_2^{\bullet-}] - k_2[Mn^{III}SOD][O_2^{\bullet-}] - k_{-5}[Mn^{III}SOD][H_2O_2] \quad (19)$$

$$\frac{d[Mn^{III}SOD : O_2^{\bullet-}]}{dt} = k_2[Mn^{III}SOD][O_2^{\bullet-}] - k_{-2}[Mn^{III}SOD : O_2^{\bullet-}] - k_3[Mn^{III}SOD : O_2^{\bullet-}] \quad (20)$$

$$\frac{d[Mn^{II}SOD]}{dt} = k_3[Mn^{III}SOD : O_2^{\bullet-}] + k_{-4}[Mn^{II}SOD : O_2^{\bullet-}] - k_4[Mn^{II}SOD][O_2^{\bullet-}] \quad (21)$$

$$\frac{d[Mn^{II}SOD : O_2^{\bullet-}]}{dt} = k_4[Mn^{II}SOD][O_2^{\bullet-}] + k_{-5}[Mn^{III}SOD][H_2O_2] + k_{-6}[DEP] - k_{-4}[Mn^{II}SOD : O_2^{\bullet-}] - k_5[Mn^{II}SOD : O_2^{\bullet}] - k_6[Mn^{II}SOD : O_2^{\bullet-}] \quad (22)$$

$$\frac{d[H_2O_2]}{dt} = k_5[Mn^{II}SOD : O_2^{\bullet-}] + 2k_7[O_2^{\bullet-}] - k_{-5}[Mn^{III}SOD][H_2O_2] - k_8[GPx_r][H_2O_2] \quad (23)$$

$$\frac{d[DEP]}{dt} = k_6[Mn^{II}SOD : O_2^{\bullet-}] - k_{-6}[DEP] \quad (24)$$

$$\frac{d[GPx_r]}{dt} = k_{10}[GSGPx][GSH] - k_8[GPx_r][H_2O_2] \quad (25)$$

$$\frac{d[GPx_0]}{dt} = k_8[GPx_r][H_2O_2] - k_9[GPx_0][GSH] \quad (26)$$

$$\frac{d[H_2O]}{dt} = k_8[GPx_r][H_2O_2] + k_9[GPx_0][GSH] \quad (27)$$

$$\frac{d[GSH]}{dt} = -k_9[GPx_0][GSH] - k_{10}[GSGPx][GSH] \quad (28)$$

$$\frac{d[GSGPx]}{dt} = k_9[GPx_0][GSH] - k_{10}[GSGPx][GSH] \quad (29)$$

$$\frac{d[GSSG]}{dt} = k_{10}[GSGPx][GSH] \quad (30)$$

10-acetyl-3,7-dihydroxyphenoxazine (ADHP) [53], using the Amplex Red Hydrogen Peroxide/Peroxidase Assay Kit (Molecular Probes, Eugene, OR). Amplex Red is considered a sensitive probe for H_2O_2, but can have interferences that can overwhelm the H_2O_2 signal of interest [54]. In the presence of H_2O_2 and horseradish peroxidase (HRP), ADHP generates a fluorescent oxidation product, resorufin, with an absorption maximum of approximately 563 nm and emission maximum around 587 nm [55]. In the assay exponentially growing cells had their growth medium replaced with a phosphate buffer (pH 7.4) and the appearance of H_2O_2 in the buffer was followed with time. The rates of appearance of H_2O_2, reflecting the intracellular $[H_2O_2]_{ss}$, are compared.

Results and discussion

MnSOD overexpression in cells results in an increase in H_2O_2

There are various cellular sources that can produce H_2O_2. As a reliable measure of cellular production of H_2O_2 we have determined the rate of accumulation of extracellular H_2O_2 from several cell types. To determine if MnSOD influences the formation of H_2O_2 we used cells that had been transfected with MnSOD cDNA. This transfection provided clones with varying levels of MnSOD. These clones have been well characterized [56–58] and their antioxidant enzyme profile was verified for these experiments. The relative MnSOD activity for the different clones ranged from the same as wild type to a 19-fold increase in MnSOD activity. CuZnSOD activity in the transfected clones was comparable to parental cells; likewise peroxide-removing ability (catalase and glutathione peroxidase) was similar. We measured the appearance of H_2O_2 in media from dividing, unstressed cells. The rate of appearance of H_2O_2 in the media increased as the activity of

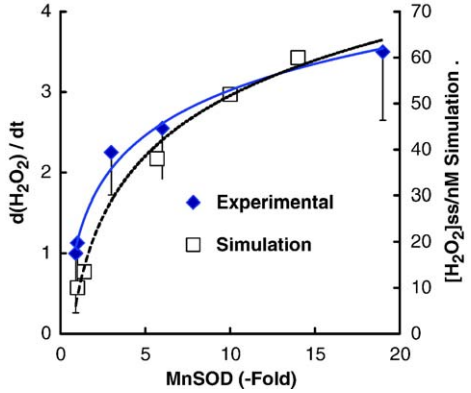

Fig. 3. The rate of accumulation of H_2O_2 in the media increases with the cellular MnSOD activity. (◆) The H_2O_2 released from MCF-7 cells and several clones overexpressing MnSOD (1.1-, 3-, 6-, and 19-fold) in exponential growth was determined at several time points over a period of two hours. The concentrations of H_2O_2 in the medium were measured using Amplex Red. The ordinate represents the change in the $[H_2O_2]$ in the media versus time compared to wildtype MCF-7 cells (1 on the left ordinate scale represents 2.8 zmol cell^{-1} s^{-1}). Results are from three independent experiments ± standard deviation. (□) The mitochondrial steady-state level of H_2O_2 (nM) from the kinetic model achieved with different levels of MnSOD (0.7–10 μM) as presented in Fig. 4D.

MnSOD increased, Fig. 3. Different MnSOD levels influenced the formation of H_2O_2 to different degrees. A 3-fold increase in MnSOD activity resulted in a 2-fold increase in the rate of accumulation of H_2O_2 in the medium, while a 19-fold increase in MnSOD, resulted only in a 3.5-fold increase in the rate of accumulation of H_2O_2. Thus, in cells with low levels of MnSOD, modest increases in MnSOD will have a greater relative impact on the rate of formation of H_2O_2 than very large increases in MnSOD.

Similar measurements were done with wild type prostate cancer cells (PC-3) and a MnSOD-overexpressing clone (8.3-fold increase in MnSOD activity). The rate of appearance of extracellular H_2O_2 was 1.9-fold higher in the transfected clone compared to wild type PC-3 cells [58]. In a second study with PC-3 cells, we found that a clone with an 8.2-fold increase in MnSOD activity produced a 1.5-fold increase in the rate of appearance of H_2O_2 in the media compared to wildtype PC-3 cells [57]. Thus, an increase in MnSOD activity increases the rate of appearance of H_2O_2 in the extracellular medium, consistent with an increase in the rate of production of intracellular H_2O_2.

Setting up the components of the kinetic model for the formation of H_2O_2

To understand how increasing the level of SOD increases the rate of production of H_2O_2 in cells (Fig. 3), we set up a kinetic model. Because the experimental results above used cells with varying levels of the mitochondrial form of SOD, MnSOD, we chose as a focus the production of superoxide by the mitochondrial electron transport chain (ETC) and compared this to the formation of $O_2^{\bullet -}$ from the X/XO system.

For the initial conditions in the model we started with all the MnSOD in its resting state of $Mn^{III}SOD$ with no H_2O_2 present, Table 3. To investigate how the rate of formation of H_2O_2 changes with [MnSOD], we varied the apparent equilibrium constant for the specific reaction that forms superoxide, Reaction (1), by changing the value of the reverse rate constant for Reaction (1), k_{-1}, and thereby changing the apparent value of the equilibrium constant for this reaction, $K_1 = 0.001–1000$. For each value of K_1 we varied the level of MnSOD from 0.7 μM–10 μM. We kept the capacity for the removal of peroxide constant. Once the system was allowed to evolve, it took on the order of 10–100 s for H_2O_2 to reach observable levels, Fig. 4. After a short time the level of H_2O_2 reaches a steady-state. The delay in the appearance of H_2O_2 is because H_2O_2 is only formed *via* the reaction of $O_2^{\bullet -}$ with $Mn^{II}SOD$, Reactions (4) and (5). Because the initial conditions had MnSOD in the oxidation state of Mn^{III}, it takes some time to convert a significant amount of $Mn^{III}SOD$ to $Mn^{II}SOD$, Reactions (2) and (3). As expected, this lag time increases with increasing initial concentration of $Mn^{III}SOD$.

For our kinetic model we have chosen concentrations of participants that are our best interpretation of the literature, Table 3. However, even if future research suggests concentrations that differ by an order of magnitude or more, the principal findings of this model still hold.

If $K_1 > 1$, e.g., XO, then SOD has no influence on the production of H_2O_2

When the rate constant for the forward reaction of Reaction (1) is greater than the rate constant for the reverse reaction, *i.e.* $k_f > k_r$ or $K_1 > 1$, then $[H_2O_2]_{ss}$ does not change with varying

Table 3
The species in the model and their initial concentrations

Species	$[Species]_i$/M [a]	Comment/Reference
$CoQ+CoQH_2$	5×10^{-4}	This concentration is based on data on rat liver mitochondria (120,000 total molecules/mitochondrion [75]; volume = 0.42 μm^3 [103]), but assumes a homogeneous distribution. If considering only the lipid phase of mitochondria, then $[CoQ_{10}]$ is estimated to be 10 times this concentration (5 mM) in this phase [104] This is comparable to information on heart mitochondria [105–107]
CoQ	4.5×10^{-4}	90% of coenzyme Q, ubiquinone, is estimated to be in the oxidized form [75], however this can be expected to vary [108].
$CoQH_2$	0.5×10^{-4}	10% of coenzyme Q is estimated to be in the reduced form [75,109].
$CoQ^{\bullet -}$	1×10^{-7}	This estimate assumes that 1 part in 5,000 of $CoQ+CoQH_2$ exists as the radical [74,110].
O_2	25×10^{-6}	
$O_2^{\bullet -}$	0	
Mn(III)SOD	Varied in the model	The resting state of MnSOD
$Mn(III)SOD:O_2^{\bullet -}$	0	An intermediate in the reduction of Mn(III)SOD
Mn(II)SOD	0	The reduced form of MnSOD. The rate production of H_2O_2 by MnSOD is maximized when [Mn(II)SOD]:Mn(III)SOD is 1:1
$Mn(II)SOD:O_2^{\bullet -}$	0	An intermediate in the oxidation of Mn(II)SOD
H_2O	55	
DEP	0	Is a dead end product, *i.e.* inactivation of MnSOD
GPx_r	1×10^{-6}	The reduced form of GPx that reacts with hydroperoxides
GPx_o	0	The oxidized form of GPx that enters into reactions with GSH to recycle back to GPx_r
H_2O_2	0	
GSH	1×10^{-3}	Glutathione
GSGPx	0	An intermediate in the reaction of GSH with GPx_o
GSSG	0	Glutathione disulfide

[a] This is the initial concentration at time zero.

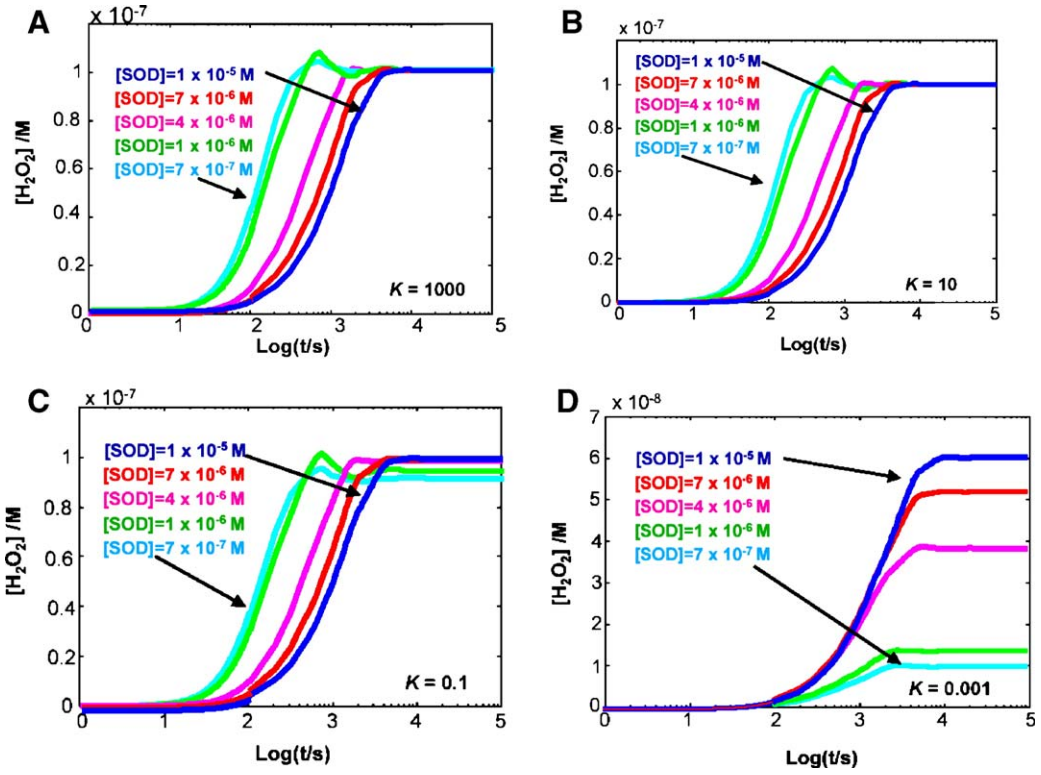

Fig. 4. The steady-state concentration of H_2O_2 in cells can be a function of the level of MnSOD. The kinetic model clearly demonstrates that when $K<1$ for Reaction (1) the level of SOD will determine the flux of H_2O_2 as well as its steady-state level. (A) $K=1000$; (B) $K=10$; (C) $K=0.1$; (D) $K=0.001$. The different values for the equilibrium constant were achieved by varying the rate constant for the reverse reaction of Reaction (1), keeping the value of the forward rate constant at 8×10^3 M^{-1} s^{-1}. In the kinetic model, the capacity to remove H_2O_2 was kept constant.

concentrations of MnSOD, Figs. 4A and 4B. When $K_1>1$, *e.g.* $K_1=1000$ (Fig. 4A), the same steady-state level of H_2O_2 is achieved for all [MnSOD] examined. This is because little of the $O_2^{\bullet-}$ formed enters into the reverse reaction, so essentially all superoxide will dismute to give H_2O_2, with or without SOD. This scenario applies for the XO-xanthine system.

The kinetics for superoxide production by X/XO is initiated by the formation of a XO-xanthine complex, Fig. 1. The actual production of superoxide is accomplished by reaction of the flavin radical of FAD, $FADH^{\bullet}$, with O_2. In the blood plasma of healthy humans typical levels of hypoxanthine are approximately 2 μM with xanthine levels on the order of only 1 μM or less [59]; these values can vary considerably. Using the rate constants of Fig. 1, a pseudo first-order rate constant for X/XO complex formation will be about 10 s^{-1}. These electrons are quickly transferred to FAD. Oxygen levels in blood of course vary, but if we assume a typical concentration to be ≈150 μM, then the pseudo first-order rate constant for the oxidation of $FADH^{\bullet}$ by oxygen to form $O_2^{\bullet-}$ will be 10 s^{-1}. This estimate shows that the rate of enzyme reduction and subsequent oxidation to form $O_2^{\bullet-}$ are about the same. Thus, SOD could have an effect on the rate of production of H_2O_2 because the oxidation of $FADH^{\bullet}$ is not necessarily rate-limiting. However, the thermodynamics of the $FADH^{\bullet}+O_2$ reaction to form $O_2^{\bullet-}$ has $K_{1a}=10^4$; see Introduction. The model predicts that SOD would have little or no effect on the rate of production of superoxide and hydrogen peroxide because of this high value for K_1.

When $K_1>1$, to change the rate of production of $O_2^{\bullet-}$, and subsequently H_2O_2, the concentration of the limiting reagents must be modulated. The limit for the rate of formation of $O_2^{\bullet-}$ in this setting is the rate of the forward reaction for Reaction (1). Thus, increasing the concentration of the radical source for $O_2^{\bullet-}$ ($FADH^{\bullet}$) or O_2 would increase the flux of $O_2^{\bullet-}$ and H_2O_2 as either $FADH^{\bullet}$ or O_2, or both, are the limiting reagents. The level of MnSOD will affect $[O_2^{\bullet-}]_{ss}$. In this kinetic model, if [MnSOD] is increased by a factor of two, the steady state level of $O_2^{\bullet-}$ decreases by a factor two, *i.e.* $[O_2^{\bullet-}]_{ss}$ will be a direct function of 1/[MnSOD], assuming there are no other significant sinks for $O_2^{\bullet-}$. However, the level of MnSOD would not affect the flux of $O_2^{\bullet-}$ and H_2O_2.

If $K_1<1$, e.g. CoQ, then SOD can influence the production of H_2O_2

When $k_f<k_r$, $K_1<1$, the steady-state level of H_2O_2 achieved is a function of the level of MnSOD, the higher [MnSOD] the greater $[H_2O_2]_{ss}$, Figs. 4C and 4D. The steady-state level of H_2O_2 will change if either its rate of removal or rate of formation changes. In the model we kept the capacity to remove H_2O_2 constant; thus, the rate of production must change. The rate of production of H_2O_2 changes in the presence of SOD because the very fast reverse reaction for Reaction (1) gives little chance for chemical dismutation of $O_2^{\bullet-}$ to H_2O_2 and O_2. The very fast reaction of SOD consumes the $O_2^{\bullet-}$ before it can enter the reverse reaction of Reaction (1). From an examination

Table 4
The pool of electrons in the ETC is large

Redox component	Molecules per inner membrane [75] [a]	% reduced/ oxidized of redox partners at steady state [75,111]	Redox e^- [112]	Number of redox electrons in pool per mitochondrion
Complex I	2000	$I(5_{red}) \rightarrow CoQ(90_{ox})$ [b]	2 [c]; 8 [d]	800
Complex II	3800	$II(5_{red}) \rightarrow CoQ(90_{ox})$	2; 4	800
CoQ	120,000	$CoQ(10_{red}) \rightarrow III(84_{ox})$	2; 2	24,000
Complex III	5700	$III(16_{red}) \rightarrow c(89_{ox})$	1; 3 [e]	2700
Cytochrome *c*	17,000	$c(11_{red}) \rightarrow IV(80_{ox})$	1; 1	1900
Complex IV	13,000	$IV(20_{red})$	4; 4	10,600
				Total=40,800
				Total in Complexes I, II and CoQ=25,000

[a] These estimates from [75] have been rounded to two-significant digits.
[b] These estimates are for uncoupled mitochondria from rat liver. The percent of reduced species will vary considerably, being greater for active mitochondria.
[c] Number of electrons transferred in turnover in the ETC.
[d] Maximum number of redox electrons that could in principal be held in each complex or redox species.
[e] This does not include CoQ.

of the slopes of the lines at ≈1000 s (log t=3) in Fig. 4D (K_I=0.001), we can see that indeed the *rate* of formation of H_2O_2 increases with increasing MnSOD. Thus, the kinetic model predicts that a change in the level of MnSOD will change the rate of production of $O_2^{\bullet -}$ and subsequently the flux of H_2O_2. This scenario applies to the CoQ-system.

The semiquinone radical ($CoQ^{\bullet -}$) of coenzyme Q (ubiquinone) of the ETC is thought to be the primary source of superoxide in most non-phagocytic cells, Fig. 2 [60–68]. A small percent (on the order of 1% or less) of the overall electron-flow through the ETC in normal, healthy cells is thought to result in the production of superoxide [67,69,70]. Values for some of the parameters in the kinetic model are sparse. To ensure that the conclusions drawn from the model are reliable, we tested wide ranges of concentrations to determine when significant changes in the outcome occurred. In the kinetic model we assumed a constant level of $CoQ^{\bullet -}$ and dioxygen [71,72]. We reasoned that the level of $CoQ^{\bullet -}$ would be in a relative steady-state in an unchanging environment because of its formation as an intermediate in the protonmotive Q cycle [68,73]; in addition CoQ and $CoQH_2$ readily comproportionate to form $2CoQ^{\bullet -}$ ($k \approx 250\ M^{-1}\ s^{-1}$; $K \approx 6 \times 10^{-5}$ [74]). Thus, any $CoQ^{\bullet -}$ lost to its reaction with O_2 to form $O_2^{\bullet -}$, Reaction (1), would be rapidly replaced.

The thermodynamics of the $CoQ^{\bullet -} + O_2$ reaction to form superoxide is considerably different than for the X/XO system. The range of ΔE for Reaction (1) with $CoQ^{\bullet -}$ as the electron source for $O_2^{\bullet -}$ yields an equilibrium constant in the range of 10^{-2} to 10^{1}. This much smaller value for K_1 allows MnSOD to change the rate of production of superoxide and H_2O_2, Fig. 3.

A pool of electrons is essential

Another difference between the CoQ system and the XO system is the size of the electron pool. Only a very small percentage (≈1% or less) [67,69,70] of the electrons passing through the electron transport chain actually result in superoxide formation. This loss of electrons from the ETC due to the increase in the rate of superoxide formation with increasing levels of SOD is only a small perturbation on the overall electron-flow through the mitochondria. The ETC has at any time more than 40,000 redox active electrons, of which 60% reside in Complexes I, II and $CoQH_2$, Table 4. This large pool of electrons in the ETC coupled with the mobility of CoQ in the mitochondrial inner membrane [75] will instantly re-establish the steady-state level of $CoQ^{\bullet -}$, because $CoQ^{\bullet -}$ is formed as an intermediate in the protonmotive Q-cycle [68,73] as well as through comproportionation of CoQ and $CoQH_2$. The system is then poised to produce yet another molecule of superoxide. This large pool of electrons is a ready source for the production of $O_2^{\bullet -}$ and H_2O_2 that can be modulated by SOD, Fig. 5.

In contrast to $CoQ^{\bullet -}$, the X/XO system has a very small pool of electrons. Each enzyme molecule can hold six electrons per subunit. X/XO makes both H_2O_2 and O_2. The ratio of products depends on pH, substrate, and substrate concentration [76]. Superoxide is formed from $FADH^{\bullet}$; this moiety exists only when XO is relatively empty of electrons [77,78]. The nearer XO is to full capacity, the greater the proportion of H_2O_2 formed. SOD will have no effect on the direct formation of H_2O_2 by XO; it will also have no effect on the production of H_2O_2 *via* superoxide.

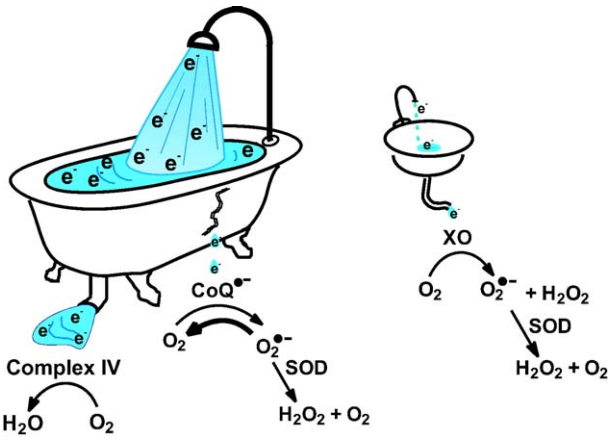

Fig. 5. The ability of SOD to modulate the flux of H_2O_2 and $[H_2O_2]_{ss}$ depends on the availability of a sufficient pool of electrons. The ETC has a large pool of electrons. The vast majority flow through complex IV to O_2 forming H_2O at the end of the ETC; a very small fraction form $O_2^{\bullet -}$. The CoQ-system has appropriate thermodynamics and access to a large pool of electrons so that MnSOD can modulate the flux of $O_2^{\bullet -}$ and subsequently H_2O_2. XO has unfavorable thermodynamics, which do not allow SOD to modulate the flux of $O_2^{\bullet -}$; in addition there is a very limited pool of electrons to draw from. Although $CoQ^{\bullet -}$ is thought to be the principal source for formation of superoxide in mitochondria, other sites may also be sources of $O_2^{\bullet -}$.

Even if the thermodynamics of a reaction are appropriate and there are no limiting reagents on the reactant side of Reaction (1), the rate of the process must be on the time-scale of the biochemistry of the cell for mass action to be of significance. Or stated another way, the magnitude of the activation energies must be appropriate to allow reactions to proceed on the time scale of the biochemistry of the cell. We evaluated the literature and chose to use a forward rate constant for the $CoQ^{\bullet -}$ system of $\approx 10^4$ M^{-1} s^{-1} for Reaction (1b), Table 1. If this rate constant were lower, *e.g.* $\approx 10^{-2}$ M^{-1} s^{-1}, and the equilibrium constant was ≈ 0.01, as with Reaction (1b), then SOD would still "pull" the reaction as per Le Chatelier's principle. However, in a biological setting and biological time scale there would be no detectable change in the flux of H_2O_2. The rate of formation of H_2O_2 would be a million times slower and would not be of consequence; The curves of Fig. 4 would be shifted from a sub-μM concentration-range to sub-pM, *i.e.* less than 1 molecule of H_2O_2 from this source in a typical cell. Thus, rate constants must be appropriate for the time scale of the process; the rate constants for Reaction (1b) are appropriate for the biological time scale.

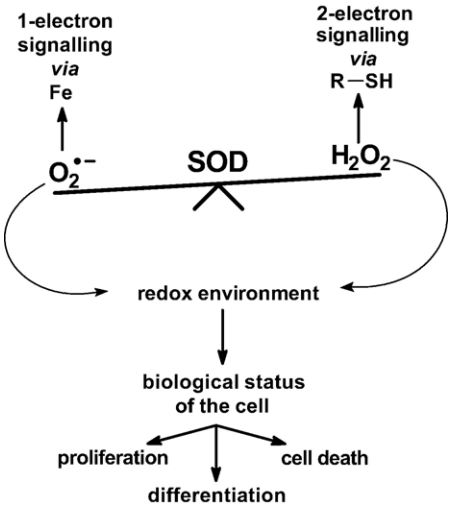

Fig. 6. MnSOD serves as a rheostat for both superoxide and hydrogen peroxide signalling. By controlling $[O_2^{\bullet -}]_{ss}$ MnSOD influences certain reactive Fe-centers in enzymes and proteins that are sensitive to oxidation/reduction by $O_2^{\bullet -}$. By changing the flux of H_2O_2, MnSOD will also modulate signalling processes that go through the thiol-system. Thus, MnSOD serves as a rheostat for both one-electron and two-electron signalling pathways. These signalling processes set the redox environment of cells, which in turn establishes the biological state of cells and tissues.

Biological implications: a new view on the function of MnSOD; when $K<1$, SOD can change $[H_2O_2]_{ss}$

The experimental results shown in Fig. 3 are consistent with our kinetic model. The MCF-7 wildtype cells have very low MnSOD activity. Increasing this activity modestly results in a large increase in the rate of appearance of H_2O_2 in the medium, but additional increases result in a smaller relative increase in H_2O_2.

Our kinetic model demonstrates that maximal $[H_2O_2]_{ss}$ is achieved when $K_1>1$. When $K_1>1$, the reverse reaction is relatively slow and the vast majority of the superoxide formed dismutes, Figs. 4A and 4B, resulting in maximal flux of $O_2^{\bullet -}$/H_2O_2. Most interesting is that when $K_1<1$, the $[H_2O_2]_{ss}$ achieved is less than the maximum possible $[H_2O_2]_{ss}$ as most of the superoxide formed is lost in the reverse reaction, Fig. 4D. Of special interest in Fig. 4D is that even when [MnSOD] = 10 μM, the steady-state level of H_2O_2 is only 60% of that when $K_1>1$, *e.g.*, Figs. 4A and 4B. When $K_1=0.001$ (Fig. 4D), it would take [MnSOD] >100 μM to approach the maximum achievable $[H_2O_2]_{ss}$. These findings on H_2O_2 are of considerable biological significance as they suggest that for cells with relatively low MnSOD, an increase in enzyme activity will produce a relatively large increase in the rate of formation of H_2O_2 and $[H_2O_2]_{ss}$. But for cells that have robust levels of MnSOD, more MnSOD will have only a minor effect on the rate of formation of H_2O_2.

These findings establish a basis for a new paradigm for the biological function of SOD. The traditional view is that by controlling the steady-state level of superoxide, SOD protects cells and tissues from potential damage. Thus, SOD is a primary antioxidant enzyme. Here we have shown how SOD can alter the flux of H_2O_2. Both, superoxide and H_2O_2 are signalling molecules. Superoxide is known to react with certain Fe-centers in enzymes while hydrogen peroxide is in general changing the sulfhydryl tone of the cell. SOD serves as a rheostat for each of these processes; an increase in MnSOD would lower $[O_2^{\bullet -}]_{ss}$ and increase $[H_2O_2]_{ss}$; thus, MnSOD could serve as the switching mechanism between one-electron signalling and two-electron signalling processes, Fig. 6. Being able to modulate the intracellular H_2O_2 flux, positions SOD as a major player in establishing the redox environment of a cell. It is thought that the redox environment of the cell is tightly connected to the biological status of the cell. Changes in the redox environment from reducing to more oxidizing can move cells through biological states such as proliferation, differentiation, and cell death [89]. H_2O_2 has been implicated in bringing about these biological changes. Thus, MnSOD could be a regulator of the cellular redox environment and with this control in part the biological state of the cell. This could explain the role of $O_2^{\bullet -}$ and MnSOD in the basic biology of proliferating cells, such as cancer cells, as well as a role for SOD in the treatment of cancer. MnSOD may have an even larger influence in pathologies that affect mitochondria.

MnSOD has been found to be low in many cancer cells [57,79–83], fetal cells [84–86], as well as stem cells [87]. Forced overexpression of MnSOD slows the growth of cancer cells both *in vitro* and *in vivo* [57,82,83,88]. These and many other studies have clearly demonstrated that MnSOD suppresses cell growth. This growth suppression could be in part a result of increasing the flux of H_2O_2 and thereby pushing the redox status of the cell to a more oxidized state. This more oxidized redox environment will no longer support cell proliferation, but rather is associated with differentiation [89–91].

Summary

The results presented here indicate that:

- the flux of H_2O_2 increases in cells as MnSOD increases;
- SOD can modulate the flux of $O_2^{\bullet -}$ and H_2O_2 only when the equilibrium constant for the reaction forming superoxide is less than or equal to ≈ 1, *e.g.* $CoQ_{10}^{\bullet -} + O_2$;
- in addition, for MnSOD to be able to influence the flux of H_2O_2, a sufficient pool of electrons is needed; the ETC has such a pool;
- the rate constant for the reaction of $CoQ^{\bullet -}$ with O_2 to form $O_2^{\bullet -}$ is of a magnitude to yield a rate of formation of H_2O_2 appropriate for the time scale of the biochemistry of the cell;
- an increase in MnSOD will lower $[O_2^{\bullet -}]_{ss}$ in proportion to 1/[MnSOD];
- an increase in MnSOD will increase the relative flux of H_2O_2 and $[H_2O_2]_{ss}$ in cells with low MnSOD more, compared to those with robust levels of MnSOD.

The results presented here suggest an entirely new function for MnSOD. MnSOD not only controls the levels of $O_2^{\bullet -}$, but it can also be viewed as an enzyme that plays a role in establishing the flux of H_2O_2 in cells. Because H_2O_2 is a key to determining the redox environment of cells and tissues, MnSOD should now be viewed not only as an antioxidant enzyme but also as a key enzyme involved in the establishment of the cellular redox environment and thereby the biological status of cells and tissues.

Acknowledgments

This work was supported in part by NIH grants CA66081 and CA81090.

References

[1] Fridovich, I. Superoxide radical and superoxide dismutases. *Annual Review of Biochemistry* **64:**97–112; 1995.
[2] Fridovich, I. Superoxide dismutases. An adaptation to a paramagnetic gas. *J. Biol. Chem.* **264:**7761–7764; 1989.
[3] Klug, D.; Rabani, J.; Fridovich, I. A direct demonstration of the catalytic action of superoxide dismutase through the use of pulse radiolysis. *J. Biol. Chem.* **247:**4839–4842; 1972.
[4] Klug-Roth, D.; Fridovich, I.; Rabani, J. Pulse radiolytic investigations of superoxide catalyzed disproportionation. Mechanism for bovine superoxide dismutase. *J. Am. Chem. Soc.* **95:**2786–2790; 1973.
[5] Bielski, B. H. J.; Cabelli, D. E.; Arudi, R. L.; Ross, A. B. Reactivity of hydroperoxyl/superoxide radicals in aqueous solution. *J. Phys. Chem. Ref. Data* **14:**1041–1100; 1985.
[6] Li, Y.; Huang, T. T.; Carlson, E. J.; Melov, S.; Ursell, P. C.; Olson, J. L.; Noble, L. J.; Yoshimura, M. P.; Berger, C.; Chan, P. H.; Wallace, D. C.; Epstein, C. J. Dilated cardiomyopathy and neonatal lethality in mutant mice lacking manganese superoxide dismutase. *Nature Genetics* **11:** 376–381; 1995.
[7] Lebovitz, R. M.; Zhang, H.; Vogel, H.; Cartwright Jr., J.; Dionne, L.; Lu, N.; Huang, S.; Matzuk, M. M. Neurodegeneration, myocardial injury, and perinatal death in mitochondrial superoxide dismutase-deficient mice. *Proc. Natl. Acad. Sci. U. S. A.* **93:**9782–9787; 1996.
[8] Scott, M. D.; Meshnick, S. R.; Eaton, J. W. Superoxide dismutase-rich bacteria. Paradoxical increase in oxidant toxicity. *J. Biol. Chem.* **262:** 3640–3645; 1987.
[9] Scott, M. D.; Meshnick, S. R.; Eaton, J. W. Superoxide dismutase amplifies organismal sensitivity to ionizing radiation. *J. Biol. Chem.* **264:** 2498–2501; 1989.
[10] Elroy-Stein, O.; Bernstein, Y.; Groner, Y. Overproduction of human Cu/Zn-superoxide dismutase in transfected cells: extenuation of paraquat-mediated cytotoxicity and enhancement of lipid peroxidation. *EMBO J.* **5:**615–622; 1986.
[11] Amstad, P.; Peskin, A.; Shah, G.; Mirault, M. -E.; Moret, R.; Zbinden, I.; Cerutti, P. The balance between Cu,Zn-superoxide dismutase and catalase affects the sensitivity of mouse epidermal cells to oxidative stress. *Biochem.* **30:**9305–9313; 1991.
[12] Teixeira, H. D.; Schumacher, R. I.; Meneghini, R. Lower intracellular hydrogen peroxide levels in cells overexpressing CuZn-superoxide dismutase. *Proc. Natl. Acad. Sci. U. S. A.* **95:**7872–7875; 1998.
[13] Li, S.; Yan, T.; Yang, J. Q.; Oberley, T. D.; Oberley, L. W. The role of cellular glutathione peroxidase redox regulation in the suppression of tumor cell growth by manganese superoxide dismutase. *Cancer Res.* **60:** 3927–3939; 2000.
[14] Zhang, H. J.; Zhao, W.; Venkataraman, S.; Robbins, M. E.; Buettner, G. R.; Kregel, K. C.; Oberley, L. W. Activation of matrix metalloproteinase-2 by overexpression of manganese superoxide dismutase in human breast cancer MCF-7 cells involves reactive oxygen species. *J. Biol. Chem.* **277:**20919–20926; 2002.
[15] Kim, K. H.; Rodriguez, A. M.; Carrico, P. M.; Melendez, J. A. Potential mechanisms for the inhibition of tumor cell growth by manganese superoxide dismutase. *Antiox Redox Signal.* **3:**361–373; 2001.
[16] Rodriguez, A. M.; Carrico, P. M.; Mazurkiewicz, J. E.; Melendez, J. A. Mitochondrial or cytosolic catalase reverses the MnSOD-dependent inhibition of proliferation by enhancing respiratory chain activity, net ATP production, and decreasing the steady state levels of H_2O_2. *Free Radic. Biol. Med.* **29:**801–813; 2000.
[17] Liochev, S. I.; Fridovich, I. The role of $O_2^{\bullet -}$ in the production of $HO^{\bullet}$: in vitro and in vivo. *Free Radic. Biol. Med.* **16:**29–33; 1994.
[18] Gardner, R.; Salvador, A.; Moradas-Ferreira, P. Why does SOD overexpression sometimes enhance, sometimes decrease, hydrogen peroxide production? A minimalist explanation. *Free Radic. Biol. Med.* **32:**1351–1357; 2002.
[19] Kowald, A.; Lehrach, H.; Klipp, E. Alternate pathways as mechanism for the negative effects associated with overexpression of superoxide dismutase. *J. Theoretical Biol.* **238:**828–840; 2006.
[20] McCord, J. M.; Fridovch, I. Superoxide dismutase: an enzymatic function for eythrocuprein (hemocuprein). *J. Biol. Chem.* **244:** 6049–6055; 1969.
[21] Misra, H. P.; Fridovich, I. The role of superoxide anion in the autoxidation of epinephrine and a simple assay for superoxide dismutase. *J. Biol. Chem.* **247:**3170–3175; 1972.
[22] Bors, W.; Michel, C.; Saran, M.; Lengfelder, E. The involvement of oxygen radicals during the autoxidation of adrenalin. *Biochim. Biophys. Acta.* **540:**162–172; 1978.
[23] Heikkila, R. E.; Cohen, G. 6-Hydroxydopamine: evidence for superoxide radical as an oxidative intermediate. *Science* **181:**456–457; 1973.
[24] Lloyd, R. V. Mechanism of the manganese-catalyzed autoxidation of dopamine. *Chem. Res. Toxicol.* **8:**111–116; 1995.
[25] Buettner, G. R. In the absence of catalytic metals, ascorbate does not autoxidize at pH 7: ascorbate as a test for catalytic metals. *J. Biochem. Biophys. Meth.* **16:**27–40; 1988.
[26] Massey, V.; Brumby, P. E.; Komai, H.; Palmer, G. Studies on milk xanthine oxidase. Some spectral and kinetic properties. *J. Biol. Chem.* **244:**1682–1691; 1969.
[27] Harrison, R. Structure and function of xanthine oxidoreductase: where are we now? *Free Radic. Biol. Med.* **33:**774–797; 2002.
[28] Meneshian, A.; Bulkley, G. B. The physiology of endothelial xanthine oxidase: from urate catabolism to reperfusion injury to inflammatory signal transduction. *Microcirculation* **9:**161–175; 2002.
[29] McCord, J. M.; Fridovich, I. The reduction of cytochrome c by milk xanthine oxidase. *J. Biol. Chem.* **243:**5753–5760; 1968.

[30] Olson, J. S.; Ballou, D. P.; Palmer, G.; Massey, V. The reaction of xanthine oxidase with molecular oxygen. *J. Biol. Chem.* **249:**4350–4362; 1974.

[31] Porras, A. G.; Olson, J. S.; Palmer, G. The reaction of reduced xanthine oxidase with oxygen. Kinetics of peroxide and superoxide formation. *J. Biol. Chem.* **256:**9096–9103; 1981.

[32] Olson, J. S.; David, P.; Ballou, D. P.; Graham Palmer, G.; Vincent Massey, V. The mechanism of action of xanthine oxidase. *J. Biol. Chem.* **249:**4363–4382; 1974.

[33] Porras, A. G.; Palmer, G. The room temperature potentiometry of xanthine oxidase. pH-dependent redox behavior of the flavin, molybdenum, and iron-sulfur centers. *J. Biol. Chem.* **257:**11617–11626; 1982.

[34] Barber, M. J.; Siegel, L. M. In: Massey, V., Williams, C. H. Eds., Magnetic Interactions Within Xanthine Oxidase in Flavins and Flavoproteins. Elsevier, North Holland,pp. 796–804; 1982.

[35] Wardman, P. Reduction potentials of one-electron couples involving free radicals in aqueous solution. *J. Chem. Ref. Data.* **18:**1637–1755; 1989.

[36] Forman, H. J.; Kennedy, J. A. Role of superoxide radical in mitochondrial dehydrogenase reactions. *Biochem. Biophys. Res. Commun.* **60:** 1044–1050; 1974.

[37] Loschen, G.; Angelo, A.; Richter, C.; Flohé, L. Superoxide radicals as precursors of mitochondrial hydrogen peroxide. *FEBS Lett.* **42:**68–72; 1974.

[38] Forman, H. J.; Kennedy, J. Superoxide production and electron transport in mitochondrial oxidation of dihydroorotic acid. *J. Biol. Chem.* **250:** 4322–4326; 1975.

[39] Turrens, J. F.; Alexandre, A.; Lehninger, A. L. Ubisemiquinone is the electron donor for superoxide formation by complex III of heart mitochondria. *Arch. Biochem. Biophys.* **237:**408–414; 1985.

[40] Giulivi, C.; Boveris, A.; Cadenas, E. The steady-state concentrations of oxygen radicals in mitochondria. In: Gilbert, D.L., Colton, C.A. Eds., Reactive Oxygen Species in Biological Systems: An Interdisciplinary Approach. Chapter 3. Kluwer Academic/Plenum Publishers, New York, pp. 77–102; 1999.

[41] DeVries, S.; Berden, J. A.; Slater, E. C. Properties of a semiquinone anion located in the QH_2:cytochrome *c* oxidoreductase segment of the mitochondrial respiratory chain. *FEBS Lett.* **122:**143–148; 1980.

[42] Sallow, A. J. Physical chemistry of semiquinones. In: Trumpower, B. L. Ed., Function of Quinones in Energy Conserving Systems. Academic Press, New York,pp. 59–72; 1982.

[43] Miki, T.; Yu, L.; Yu, C. A. Characterization of ubisemiquinone radicals in succinate-ubiquinone reductase. *Arch. Biochem. Biophys.* **293:**61–66; 1992.

[44] Ohnishi, T.; Trumpower, B. L. Differential effects of antimycin on ubisemiquinone bound in different environments in isolated succinate cytochrome c reductase complex. *J. Biol. Chem.* **255:**3278–3284; 1980.

[45] Shampine, L. F.; Reichelt, M. W. The MATLAB ODE suite. *SIAM J. Sci. Computing* **18:**1–22; 1997.

[46] Chance, B.; Sies, H.; Boveris, A. Hydroperoxide metabolism in mammalian organs. *Physiol. Rev.* **59:**527–605; 1979.

[47] Giulivi, C.; Hochstein, P.; Davies, K. J. Hydrogen peroxide production by red blood cells. *Free Radic. Biol. Med.* **16:**123–129; 1994.

[48] Boveris, A.; Cadenas, E. Cellular sources and steady-state levels of reactive oxygen species. In: Clerch, L. B., Massaro, D. J. Eds., Oxygen, Gene Expression, and Cellular Function. Lung Biology in Health and Disease, vol. 205. Marcell Dekker, Inc, New York,pp. 1–26; 1997.

[49] Johnson, R. M.; Goyette Jr., G.; Ravindranath, Y.; Ho, Y. S. Hemoglobin autoxidation and regulation of endogenous H_2O_2 levels in erythrocytes. *Free Radic. Biol. Med.* **39:**1407–1417; 2005.

[50] Dick, D. A. The permeability coefficient of water in the cell membrane and the diffusion coefficient in the cell interior. *J. Theoretical. Biol.* **7:** 504–531; 1964.

[51] Pfeuffer, J.; Flögel, U.; Dreher, W.; Leibfritz, D. Restricted diffusion and exchange of intracellular water: theoretical modelling and diffusion time dependence of 1H NMR measurements on perfused glial cells. *MNR Biomed* **11:**19–31; 1998.

[52] Quirk, J. D.; Bretthorst, G. L.; Duong, T. Q.; Snyder, A. Z.; Springer Jr., C. S.; Ackerman, J. J.; Neil, J. J. Equilibrium water exchange between the intra- and extracellular spaces of mammalian brain. *Magnetic Resonance Med.* **50:**493–499; 2003.

[53] Zhou, M.; Diwu, Z.; Panchuk-Voloshina, N.; Haugland, R. P. A stable nonfluorescent derivative of resorufin for the fluorometric determination of trace hydrogen peroxide: applications in detecting the activity of phagocyte NADPH oxidase and other oxidases. *Anal. Biochem.* **253:** 162–168; 1997.

[54] Votyakova, T. V.; Reynolds, I. J. Detection of hydrogen peroxide with Amplex Red: interference by NADH and reduced glutathione auto-oxidation. *Arch. Biochem. Biophys.* **431:**138–144; 2004.

[55] Gutheil, W. G.; Stefanova, M. E.; Nicholas, R. A. Fluorescent coupled enzyme assays for D-alanine: application to penicillin-binding protein and vancomycin activity assays. *Anal. Biochem.* **287:**196–202; 2000.

[56] Zhang, H. J.; Yan, T.; Oberley, T. D.; Oberley, L. W. Comparison of effects of two polymorphic variants of manganese superoxide dismutase on human breast MCF-7 cancer cell phenotype. *Cancer Res.* **59:**6276–6283; 1999.

[57] Venkataraman, S.; Jiang, X.; Weydert, C. J.; Zhang, Y.; Zhang, H. J.; Goswami, P. C.; Ritchie, J. M.; Oberley, L. W.; Buettner, G. R. Manganese superoxide dismutase overexpression inhibits the growth of androgen-independent prostate cancer cells. *Oncogene* **24:**77–89; 2005.

[58] Venkataraman, S.; Wagner, B. A.; Jiang, X.; Wang, H. P.; Schafer, F. Q.; Ritchie, J. M.; Burns, C. P.; Oberley, L. W.; Buettner, G. R. Overexpression of manganese superoxide dismutase promotes the survival of prostate cancer cells exposed to hyperthermia. *Free Rad. Res.* **38:**1119–1132; 2004.

[59] Lartigue-Mattei, C.; Chabard, J. L.; Bargnoux, H.; Petit, J.; Berger, J. A.; Ristori, J. M.; Bussiere, J. L.; Catilina, P.; Catilina, M. J. Plasma and blood assay of xanthine and hypoxanthine by gas chromatography-mass spectrometry: physiological variations in humans. *J. Chrom.* **529:** 93–101; 1990.

[60] Boveris, A.; Cadenas, E.; Stoppani, A. O. Role of ubiquinone in the mitochondrial generation of hydrogen peroxide. *Biochem. J.* **156:** 435–444; 1976.

[61] Cadenas, E.; Boveris, A.; Ragan, C. I.; Stoppani, A. O. Production of superoxide radicals and hydrogen peroxide by NADH-ubiquinone reductase and ubiquinol-cytochrome c reductase from beef-heart mitochondria. *Arch. Biochem. Biophys.* **180:**248–257; 1977.

[62] Boveris, A. Mitochondrial production of superoxide radical and hydrogen peroxide. *Adv. Exp. Med. Biol.* **78:**67–82; 1977.

[63] Boveris, A. Determination of the production of superoxide radicals and hydrogen peroxide in mitochondria. *Meth. Enzymol.* **105:**429–435; 1984.

[64] Turrens, J. F.; Alexandre, A.; Lehninger, A. L. Ubisemiquinone is the electron donor for superoxide formation by complex III of heart mitochondria. *Arch. Biochem. Biophys.* **237:**408–414; 1985.

[65] Forman, H. J.; Kennedy, J. Dihydroorotate-dependent superoxide production in rat brain and liver. A function of the primary dehydrogenase. *Arch. Biochem. Biophys.* **173:**219–224; 1976.

[66] James, A. M.; Smith, R. A.; Murphy, M. P. Antioxidant and prooxidant properties of mitochondrial Coenzyme Q. *Arch. Biochem. Biophys.* **423:** 47–56; 2004.

[67] St-Pierre, J.; Buckingham, J. A.; Roebuck, S. J.; Brand, M. Topology of superoxide production from different sites in the mitochondrial electron transport chain. *J. Biol. Chem.* **277:**44784–44790; 2002.

[68] Turrens, J. F. Mitochondrial formation of reactive oxygen species. *J. Physiol.* **552:**335–344; 2003.

[69] Boveris, A.; Oshino, N.; Chance, B. The cellular production of hydrogen peroxide. *Biochem. J.* **128:**617–630; 1972.

[70] Turrens, J. F.; Boveris, A. Generation of superoxide anion by the NADH dehydrogenase of bovine heart mitochondria. *Biochem. J.* **191:**421–427; 1980.

[71] Robiolio, M.; Rumsey, W. L.; Wilson, D. F. Oxygen diffusion and mitochondrial respiration in neuroblastoma cells. *Am. J. Physiol.* **256:** C1207–C1213; 1989.

[72] Jones, D. P. Intracellular diffusion gradients of O_2 and ATP. *Am. J. Physiol.* **250:**C663–C675; 1986.

[73] Trumpower, B. L. The protonmotive Q cycle. *J. Biol. Chem.* **265:** 11409–11412; 1990.
[74] Audi, S. H.; Zhao, H.; Bongard, R. D.; Hogg, N.; Kettenhofen, N. J.; Kalyanaraman, B.; Dawson, C. A.; Merker, M. P. Pulmonary arterial endothelial cells affect the redox status of coenzyme Q_0. *Free. Radic. Biol. Med.* **34:**892–907; 2003.
[75] Hackenbrock, C. R. The random collision model and a critical assessment of diffusion and collision in mitochondrial electron transport. *J. Bioenerg. Biomembranes* **18:**331–368; 1986.
[76] Fridovich, I. Quantitative aspects of the production of superoxide anion radical by milk xanthine oxidase. *J. Biol. Chem.* **245:**4053–4057; 1970.
[77] Nishino, T. The conversion of xanthine dehydrogenase to xanthine oxidase and the role of the enzyme in reperfusion injury. *J. Biochem.* **116:**1–6; 1994.
[78] Nishino, T.; Nishino, T.; Schopfer, L. M.; Massey, V. The reactivity of chicken liver xanthine dehydrogenase with molecular oxygen. *J. Biol. Chem.* **264:**2518–2527; 1989.
[79] Oberley, L. W.; Buettner, G. R. The role of superoxide dismutase in cancer: a review. *Cancer Res.* **39:**1141–1149; 1979.
[80] Yang, J.; Lam, E. W.; Hammad, H. M.; Oberley, T. D.; Oberley, L. W. Antioxidant enzyme levels in oral squamous cell carcinoma and normal human oral epithelium. *J. Oral. Pathol. Med.* **31:**71–77; 2002.
[81] Allen, R. G.; Balin, A. K. Effects of oxygen on the antioxidant responses of normal and transformed cells. *Exp. Cell Res.* **289:**307–316; 2003.
[82] Weydert, C.; Roling, B.; Liu, J.; Hinkhouse, M. M.; Ritchie, J. M.; Oberley, L. W.; Cullen, J. J. Suppression of the malignant phenotype in human pancreatic cancer cells by the overexpression of manganese superoxide dismutase. *Molec. Cancer Ther.* **2:**361–369; 2003.
[83] Darby-Weydert, C. J.; Smith, B. B.; Xu, L.; Kregel, K. C.; Ritchie, J. M.; Davis, C. S.; Oberley, L. W. Inhibition of oral cancer cell growth by adenovirus MnSOD plus BCNU treatment. *Free Radic. Biol. Med.* **34:** 316–329; 2003.
[84] Allen, B. P.; Keogh, R. G.; Gerhard, G.; Pignolo, R.; Horton, J.; Cristofalo, V. J. Expression and regulation of SOD activity in human skin fibroblasts from donors of different ages. *J. Cell Physiol.* **165:**576–587; 1995.
[85] Allen, R. G.; Balin, A. K. Developmental changes in the superoxide dismutase activity of human skin fibroblasts are maintained in vitro and are not caused by oxygen. *J. Clin. Invest.* **82:**731–734; 1988.
[86] Balin, A. K.; Pratt, L.; Allen, R. G. Effects of ambient oxygen concentration on the growth and antioxidant defenses of human cell cultures established from fetal and postnatal skin. *Free Radic. Biol. Med.* **32:**257–267; 2002.
[87] Oberley, T. D.; Sempf, J. M.; Oberley, L. W. Immunohistochemical localization of antioxidant enzymes during hamster kidney development. *Histochem. J.* **27:**575–586; 1995.
[88] Oberley, L. W. Mechanism of the tumor suppressive effect of MnSOD overexpression. *Biomed Pharmacotherapy* **59:**143–148; 2005.
[89] Schafer, F. Q.; Buettner, G. R. Redox environment of the cell as viewed through the redox state of the glutathione disulfide/glutathione couple. *Free Radic. Biol. Med.* **30:**1191–1212; 2001.
[90] Jones, D. P. Redox potential of GSH/GSSG couple: assay and biological significance. *Meth. Enzymol.* **348:**93–112; 2002.
[91] Allen, R. G.; Newton, R. K.; Sohal, R. S.; Shipley, G. L.; Nations, C. Alterations in superoxide dismutase, glutathione, and peroxides in the plasmodial slime mold Physarum polycephalum during differentiation. *J. Cell Physiol.* **125:**413–419; 1985.
[92] Patel, K. B.; Willson, R. L. Semiquinone free radicals and oxygen. Pulse radiolysis study of one electron transfer equilibria. *J. Chem. Soc. Faraday Transactions* **69:**814–825; 1973.
[93] Sugioka, K.; Nakano, . M.; Totsune-Nakano, H.; Minakami, H.; Tero-Kubota, S.; Ikegami, Y. Mechanism of O_2^- generation in reduction and oxidation cycle of ubiquinones in a model of mitochondrial electron transport systems. *Biochim. Biophys. Acta.* **936:**377–385; 1988.
[94] Sawada, Y.; Iyanagi, T.; Yamazaki, I. Relation between redox potentials and rate constants in reactions coupled with the system oxygen-superoxide. *Biochem.* **14:**3761–3764; 1975.
[95] Pick, M.; Rabani, J.; Yost, F.; Fridovich, I. The catalytic mechanism of the manganese-containing superoxide dismutase of *Escherichia coli* studied by pulse radiolysis. *J. Am. Chem. Soc.* **96:**7329–7333; 1974.
[96] Bull, C.; Niederhoffer, E. C.; Yoshida, T.; Fee, J. A. Kinetic studies of superoxide dismutases: properties of the manganese-containing protein from *Thermus thermophilus*. *J. Am. Chem. Soc.* **113:** 4069–4076; 1991.
[97] Flohé, L.; Loschen, G.; Gunzler, W. A.; Eichele, E. Glutathione peroxidase, V. The kinetic mechanism. *Hoppe-Seylers Zeitschrift fur Physiologische Chemie.* **353:**987–999; 1972.
[98] Flohé, L. Glutathione peroxidase: fact and fiction. *Ciba Foundation Symposium.* **65:**95–122; 1978.
[99] Salvador, A.; Antunes, F.; Pinto, R. E. Kinetic modelling of in vitro lipid peroxidation experiments-'low level' validation of a model of in vivo lipid peroxidation. *Free Rad. Res.* **23:**151–172; 1995.
[100] Brandt, U. Bifurcated ubiquinone oxidation in the cytochrome bc1 complex by proton-gated charge transfer. *FEBS Lett.* **387:**1–6; 1996.
[101] Gardner, P. R.; Raineri, I.; Epstein, L. B.; White, C. W. Superoxide radical and iron modulate aconitase activity in mammalian cells. *J. Biol. Chem.* **270:**13399–13405; 1995.
[102] Poderoso, J. J.; Lisdero, C.; Schopfer, F.; Riobo, N.; Carreras, M. C.; Cadenas, E.; Boveris, A. The regulation of mitochondrial oxygen uptake by redox reactions involving nitric oxide and ubiquinol. *J. Biol. Chem.* **274:**37709–37716; 1999.
[103] Gear, A. R. L.; Bednarek, J. M. Direct counting and sizing of mitochondria in solution. *J. Cell Biol.* **54:**325–345; 1972.
[104] Rich, P. A physicochemical model of quinone-cytochrome b-c complex electron transfers. In: Trumpower, B.L. Ed., Function of Quinones in Energy Conserving Systems. Academic Press, New York, pp. 73–83; 1982.
[105] Vendelin, M.; Kongas, O.; Saks, V. Regulation of mitochondrial respiration in heart cells analyzed by reaction-diffusion model of energy transfer. *Am. J. Physiol. Cell Physiol.* **278:**C747–C764; 2000.
[106] Korzeniewski, B.; Zoladz, J. A. A model of oxidative phosphorylation in mammalian skeletal muscle. *Biophys. Chem.* **92:**17–34; 2001.
[107] Beard, D. A. A biophysical model of the mitochondrial respiratory system and oxidative phosphorylation. *PLOS Computational Biology* **1:**e36; 2005.
[108] Galinier, A.; Carriere, A.; Fernandez, Y.; Bessac, A. M.; Caspar-Bauguil, S.; Periquet, B.; Comtat, M.; Thouvenot, J. P.; Casteilla, L. Biological validation of coenzyme Q redox state by HPLC-EC measurement: relationship between coenzyme Q redox state and coenzyme Q content in rat tissues. *FEBS Lett.* **578:**53–57; 2004.
[109] Wang, Q.; Lee, B. L.; Ong, C. N. Automated high-performance liquid chromatographic method with precolumn reduction for the determination of ubiquinol and ubiquinone in human plasma. *J. Chrom. B, Biomed Sci. Appl.* **726:**297–302; 1999.
[110] Backstrom, D.; Norling, B.; Ehrenberg, A.; Ernster, L. Electron spin resonance measurement on ubiquinone-depleted and ubiquinone-replenished submitochondrial particles. *Biochim. Biophys. Acta.* **197:**108–111; 1970.
[111] Klingenberg, M.; Kröger, A. On the role of ubiquinone in the respiratory chain. In: Slater, E. C.; Kaniuga, Z.; Wojtczak, L. eds. *Biochemistry of Mitochondria*. New York: Academic Press; 1967: 11–27.
[112] Tyler, D. D. The Mitochondrion in Health and Disease. VCH Publishers, New York, NY; 1992.